Gas Sensors

DOI: 10.1002/anie.201004499

The Structure and Behavior of Platinum in SnO_2-Based Sensors under Working Conditions**

*Michael Hübner, Dorota Koziej, Matthias Bauer, Nicolae Barsan, Kristina Kvashnina, Marta D. Rossell, Udo Weimar, and Jan-Dierk Grunwaldt**

Semiconducting metal oxide based gas sensors play a tremendous role in various applications that range from comfort to safety and to process monitoring. The material of choice for reducing gases is SnO_2, which dominates not only current academic research but also commercial sensors.[1] To improve sensitivity, selectivity, and stability and to decrease the operation temperature, SnO_2 is usually doped with noble metals such as Pd, Pt, or Au.[2]

Although many efforts have been undertaken to understand the structure of these promoters, their interaction with the background and target gases and sensing, and their structure under operating conditions is still a matter of strong discussion.[3] This requires studies under real operating conditions, as has been reported in particular for catalytic studies.[4] Recent studies on the role of Pd in realistic sensors have further questioned often-anticipated mechanisms, such as spillover and Fermi control.[5]

One of the most often-used dopants especially in commercial sensors is platinum, and although several studies have focused on the oxidation state of platinum,[2b,6] none of them have focused on realistic Pt-doped SnO_2 sensors under operating conditions to allow structure–property relationships to be determined. This deficiency is due to the following challenges: 1) platinum is only present in very low concentrations (0.2–1 wt % Pt in SnO_2); 2) the layer is highly porous and only 50 μm thick, 3) platinum is usually present in much higher concentrations in the heater and the electrodes; and 4) characterization techniques that allow the identification of the structure (oxidation state, particle size, Pt composites) also in its amorphous state (short-range-order structural information) are required. XANES (X-ray absorption near-edge structure) and EXAFS (extended X-ray absorption fine structure) spectroscopy are well-established element-specific methods for this purpose, but to date, only structural characterizations before and after the reaction of the powder itself (no "operando" conditions) or idealized materials have been reported in those studies.[2b,6] Therefore, a completely new approach is required concerning the design of the sensors and the X-ray spectroscopic approach.

To decouple the XAS signal for the minute amounts of Pt ($\ll$1 wt %) in the SnO_2 matrix from the platinum-containing electrodes and heater, the electrodes and heater were replaced by metals/alloys with similar electrical/resistive properties. Au was used instead of Pt for the electrodes and Ag/Pd alloy was used for the heater (Figure 1 A). The performance of the modified sensors was verified and was very similar to the conventional systems. Furthermore, the so-called HERFD-XANES (high-energy-resolution fluorescence-detection XANES[7]) method using an X-ray emission spectrometer was used to isolate the Pt L_3 XAS signal from the underlying signals of the Au electrodes (fluorescence lines are at 9.442 and 9.713 keV, respectively). In fact, this combination of design and new spectroscopic methods not only allows the platinum-dopant structure to be determined specifically for the element, but also to record high-resolution XANES data owing to minimization of core–hole lifetime broadening,[8] which is necessary to detect subtle structural changes of the Pt centers. Furthermore, this approach paves the way to collect "range-extended" EXAFS data,[7] which is important for the structural analysis near the Pt centers.

The advantage of this approach compared to conventional fluorescence EXAFS is demonstrated in Figure 1 B. The absorption at the Pt L_3 edge is very low in comparison to the absorption at Au L_3 edge from the underlying electrodes (spectrum b). Detection of the Pt L_3 X-ray absorption spectrum by monitoring the Pt $L\alpha_1$ emission line using crystal analyzers (see the Supporting Information) suppressed the influence of undesired Au L_3 absorption edge in the EXAFS region. In Figure 1 B, the HERFD-XANES spectra at the Pt L_3 edge of the 0.2 wt % Pt:SnO_2 sensor, equipped with the Au electrodes and the Ag/Pd heater (spectrum a), is compared with those of a 25 μm thick Pt foil (spectrum d) and a

[*] Dr. M. Bauer, Prof. Dr. J.-D. Grunwaldt
Institute for Chemical Technology and Polymer Chemistry
Karlsruhe Institute of Technology (KIT)
Kaiserstrasse 12, 76128 Karlsruhe (Germany)
E-mail: grunwaldt@kit.edu
M. Hübner, Dr. N. Barsan, Prof. U. Weimar
Faculty of Mathematics and Natural Sciences
Department of Chemistry
Tübingen University, 72076 Tübingen (Germany)
Dr. D. Koziej,[+] Dr. M. D. Rossell
Department of Materials, ETH Zurich
Wolfgang Pauli Strasse 10, 8093 Zurich (Switzerland)
Dr. K. Kvashnina
ESRF, BP220
6 rue Jules Horowitz, 38043 Grenoble (France)
[+] Present address: Harvard University
School of Engineering and Applied Science
29 Oxford St., Cambridge, MA 02138 (USA)

[**] We thank ESRF (Grenoble) for beamtime allocation at the insertion device beamline ID26 and for financial support, and Dr. Pieter Glatzel for his help and discussion during the setup of the in situ HERFD-XAS and range-extended EXAFS experiments. The TEM measurements were performed at the Electron Microscopy Centre of the Swiss Institute of Technology (EMEZ).

Supporting information for this article (details on sample preparation, spectroscopic techniques, and data analysis) is available on the WWW under http://dx.doi.org/10.1002/anie.201004499.

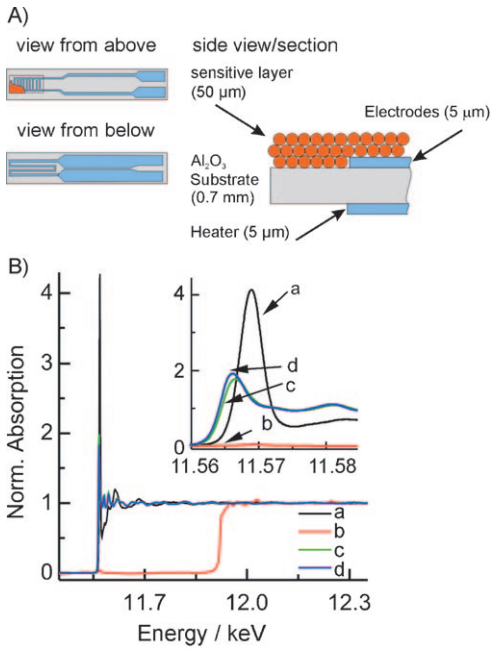

Figure 1. A) The SnO_2-based sensor equipped with electrodes and heaters. To obtain structural information of the Pt dopants on an atomic level, the conventional Pt electrodes and heater where exchanged with Au and Ag/Pd. B) Pt L_3 edge EXAFS spectra of the 0.2 wt% Pt:SnO_2 sensor with Au electrodes measured by a) HERFD and b) the traditional detection mode; for comparison, HERFD-XANES reference spectra of sensors with Pt electrodes (c) and Pt foil (d) are shown. Note the increased whiteline intensity compared to conventional XANES owing to the HERFD detection mode.

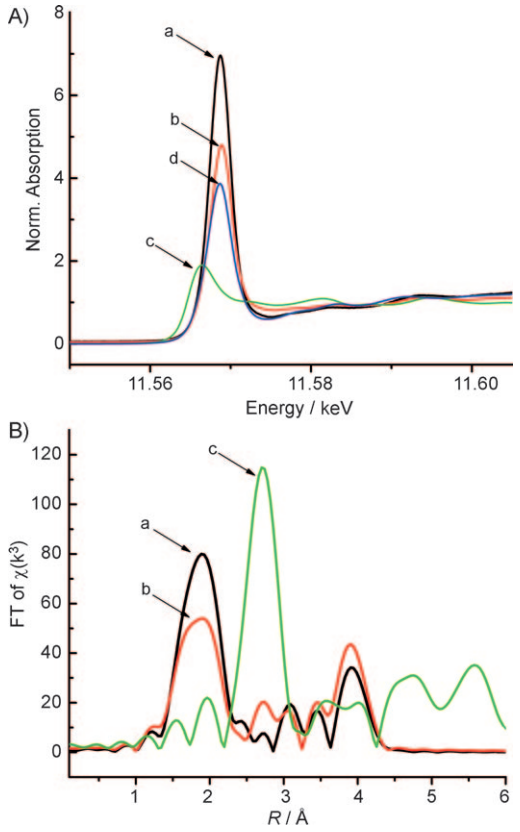

Figure 2. A) XANES spectrum of the 0.2 wt% Pt:SnO_2 sensor with a) Au electrodes in dry air at 300 °C, b) after reducing conditions (2 vol% H_2/He at 600 °C), c) SnO_2 with Pt electrodes at 300 °C in air, and d) PtO_2 powder. B) Corresponding Fourier-transformed EXAFS.

SnO_2 sensor based on the conventional substrates with Pt electrodes/heater (spectrum c). The Pt L_3 spectrum of the sensor equipped with Pt electrodes and heater, where the average of both the Pt in the SnO_2 layer and the Pt from the electrodes are detected, is almost identical to the Pt foil. However, they differ significantly from the spectrum of the 0.2 % wt Pt:SnO_2 sensor equipped with Au electrodes and Ag/Pd heater; where only the dispersed Pt in the SnO_2 layer is detected (Figure 1 B, inset). Consequently, the Pt from the electrodes is predominantly in a metallic state, which is in contrast to conclusions presented previously.[9] The whiteline intensity, which is the first resonance after the edge jump, of the Pt foil and also of the Pt electrodes is twice that of conventional spectra as lifetime broadening is suppressed in the HERFD-XANES spectra.[10] A rise in the whiteline is observed with increasing oxidation state of platinum owing to an increase of unoccupied $5d_{5/2}$ states to which the $2p_{3/2}$ core-level electron is excited.[8] Therefore, if the whiteline intensity decreases, the density of unoccupied d states is lower, which corresponds to the lower oxidation/less ionic state of Pt. The whiteline feature at 11.569 keV with peak intensity higher than 4 is characteristic for oxidized platinum with rather strong empty d states.[11] In fact, the comparison with PtO_2 reference spectra showing lower whiteline intensity than the Pt incorporated in the SnO_2 matrix (Figure 2 A) demonstrates that Pt in the SnO_2 has more empty states than Pt in PtO_2 and more electrons are transferred from the Pt to the SnO_2.

These findings from the XANES data in Figure 2 A are further supported by EXAFS data. The corresponding Fourier-transformed EXAFS spectra of the Pt sensors with special heater and electrodes (spectrum a and b) and the conventional sensor (spectrum c) are given in Figure 2 B. Whereas the conventional design only elucidates metallic Pt (from the electrode, backscattering amplitude at 2.8 Å), the main contribution in the radial distribution functions of the Fourier-transformed EXAFS of the specially designed 0.2 wt % Pt:SnO_2-based sensors is due to backscattering by the oxygen neighbors located roughly at 2.03 Å (for details of the EXAFS analysis, see the Supporting Information, Table SI-1). This observation and the absence of a Pt–Pt contribution that would be characteristic for metallic platinum or small platinum clusters (Figure 2 B c and Ref. [12]) support the fact that Pt is fully oxidized. Furthermore, two additional tin shells could be fitted at about 2.90 and 3.68 Å (Supporting Information, Table SI-1). The obtained Pt-O and Pt-Sn distances are in good agreement with the Sn-O and Sn-Sn distances of SnO_2 (see the Supporting Information). Thus, the doping of the metal oxide probably leads to substitution of Sn ions by Pt ions in the SnO_2 lattice. The high stability of the ionic platinum species in the lattice of the oxide was further established by experiments involving reduction of the sensor in 2 vol % H_2 in He at 600 °C. FT-EXAFS spectra of 0.2 wt % Pt:SnO_2 sensors before and after reduction were compared

with the spectrum of the Pt electrodes and still show the lack of Pt–Pt contributions (Figure 2B).

To determine the state of the Pt under the working conditions of the sensors, the XAS spectra and resistance changes of 0.2 wt% Pt:SnO_2 sensors were simultaneously recorded during target-gas exposure (Figure 3). Although the

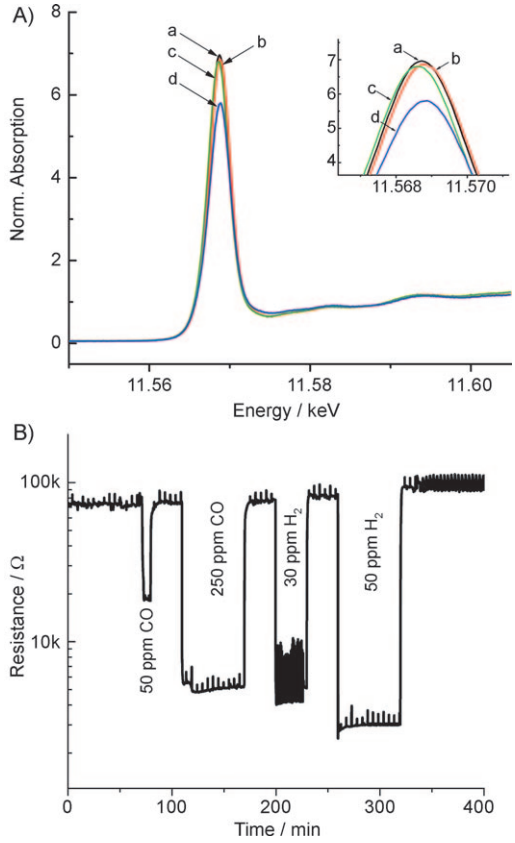

Figure 3. A) XANES of the 0.2 wt% Pt:SnO_2 sensor with Au electrodes at a) 300 °C in dry air, b) exposure to 50 ppm H_2, and c) exposure to 250 ppm CO; d) the spectra for 2 vol% H_2 in He at 400 °C for comparison. B) Resistance change of 0.2 wt% Pt:SnO_2 sensor upon exposure to 50 and 250 ppm CO and 30 and 50 ppm H_2 in dry air at 300 °C during simultaneous XANES measurements.

HERFD-XANES mode is very sensitive to subtle variations of the oxidation state, the electronic structure, or the local environment of Pt, only minor changes during the exposure to CO or H_2 in air were observed (Figure 3A), whereas huge changes in the resistance were detected (Figure 3B). This observation is further supported by EXAFS analysis in which the surrounding of Pt remains unchanged (see for example Figure 2B). The slight decrease of the whiteline intensity indicates the changes of the electronic structure induced by adsorbed CO or H_2 species, which is also known from conventional XAS.[13]

Metallic Pt particles or clusters can therefore be excluded as a reason for improved sensor activity in platinum-doped SnO_2 sensors. In fact, even in rather strong reducing conditions, no metallic Pt is observed, which is in line with HRTEM investigations that showed no Pt particles, neither before nor after reduction (see the Supporting Information). Thus, platinum seems to either influence the electronic structure as a whole and/or creates new adsorption sites in the SnO_2 lattice that leads to enhanced selectivity and sensitivity. The strong whiteline of the Pt L_3 edge and its incorporation into the lattice indicate that electrons are donated from the d band into SnO_2, changing the Fermi level and the electronic properties of SnO_2. The role played by Pt in gas sensing is therefore more complex than anticipated: On one hand, we still have, as in the case of Pd,[5] generation of further atomic/molecular adsorption sites for oxygen that are induced by the presence of Pt atoms dispersed at the surface; herein, we provide direct experimental evidence for this molecular dispersion and its consequences for the understanding of sensing. On the other hand, there is an astonishing bulk effect (in fact a Pt bulk doping), which results in more electrons in the conduction band of SnO_2. These electrons are essential for sensing because the ionosorption of oxygen at the surface of the tin dioxide requires electrons from the bulk; the formed species are the reaction partners for the reaction with reducing gases, such as H_2 and CO, and consequently the more extensive availability of these electrons contributes to the increased sensor signals.

In conclusion, new insight into the structure of the Pt constituent of SnO_2-based sensors has been achieved by high-energy-resolution fluorescence-detected X-ray absorption spectroscopy at dopant levels down to 0.2 wt% Pt and in a thin highly porous layer. For this purpose, a novel approach for identification of the sensing mechanism under working conditions was presented. First, the sensor was modified such that platinum was only present in the sensing layer. Second, the gold fluorescence was efficiently eliminated by using the high-energy-resolution fluorescence-detection mode. This procedure not only resulted in proper XANES but even in range-extended EXAFS data, as the sensor layer is located on top of the gold electrode. In this way, the study demonstrates the potential of using new synchrotron-based techniques in solid-state chemistry and materials science together with sample design and structure–function relationships. The whiteline intensity of much more than 6 revealed that platinum is in a highly oxidized state. Platinum is furthermore very difficult to reduce, which shows that it is strongly incorporated into the matrix, as also supported by detailed EXAFS analysis. These results are surprising because in many cases, metallic Pt particles or clusters have been ascribed to the improved properties. The present results reveal however that, along with the appearance of surface adsorption sites associated to the Pt atoms incorporated into the surface lattice of SnO_2, there is also a possible bulk sensitization effect linked to the increase of the free charge carriers concentrations owing to the Pt d electrons transferred to SnO_2. These conclusions on the role of Pt in Pt-SnO_2-based sensors in gas-detection mechanisms go in a similar direction as in the case of Pd in Pd-SnO_2-based sensors. However, Pd species in SnO_2 are easier to reduce than the corresponding Pt species incorporated in the SnO_2 lattice. In future, it will be rewarding applying this technique for platinum-based sensors prepared in other ways to shed even more insight into the role of surface and bulk doping and also the importance of the choice of noble metal.

Experimental Section

The investigated material was synthesized by conventional wet-chemistry sol–gel procedure. The doping was achieved by gel impregnation in the intentional concentration of $PtCl_4$. The sensors were prepared by screen-printing a paste onto an alumina substrate (a detailed description is given in Ref. [14]). High-energy-resolution fluorescence detection experiments were performed at beamline ID26 at the European Synchrotron Radiation Facility.[15] The incident energy was selected using the $<111>$ reflection from a silicon double-crystal monochromator. Rejection of higher harmonics was achieved by three Si mirrors with a Pd and Cr layers working at 2.5 mrad angle relative to the incident beam under total reflection. The energy calibration was performed on Pt foil. The incident X-ray beam had a flux of about 2×10^{13} photons per second on the sample position. HERFD-XANES spectra were measured with an X-ray emission spectrometer in the horizontal plane.[8] Sample, analyzer crystal, and photon detector (avalanche photodiode) were arranged in a vertical Rowland geometry.[16] The Pt HERFD-XANES spectra at the L_3 edge were obtained by recording the intensity of the Pt $L\alpha_1$ emission line (9442 eV) as a function of the incident energy. The emission energy was selected using the $<660>$ reflection of four spherically bent Ge crystal analyzers (with $R=1$ m) aligned at a 80° Bragg angle. A combined (incident convoluted with emitted) energy resolution of 1.8 eV was obtained as determined by measuring the elastic peak (see the Supporting Information). The sensor chamber for simultaneous XAS and resistance measurements and gas-mixing setup are described in Reference [5].

Received: July 22, 2010
Revised: September 22, 2010
Published online: February 21, 2011

Keywords: EXAFS · gas sensors · platinum · tin oxide · XANES

[1] a) K. Ihokura, J. Waston, *The Stannic Oxide Gas Sensor: Principle and Application*, CRC Press, Boca Raton, **1994**, p. 187; b) N. Barsan, M. Schweizer-Berberich, W. Gopel, *Fresenius J. Anal. Chem.* **1999**, *365*, 287; c) D. Kohl, *J. Phys. D* **2001**, *34*, R125.

[2] a) S. Capone, P. Siciliano, F. Quaranta, R. Rella, M. Epifani, L. Vasanelli, *Sens. Actuators B* **2001**, *77*, 503; b) L. Madler, T. Sahm, A. Gurlo, J. D. Grunwaldt, N. Barsan, U. Weimar, S. E. Pratsinis, *J. Nanopart. Res.* **2006**, *8*, 783; c) A. V. Tadeev, G. Delabouglise, M. Labeau, *Mater. Sci. Eng. B* **1998**, *57*, 76; d) N. Yamazoe, *Sens. Actuators B* **1991**, *5*, 7.

[3] a) N. Barsan, D. Koziej, U. Weimar, *Sens. Actuators B* **2007**, *121*, 18; b) A. Gurlo, R. Riedel, *Angew. Chem. Int. Ed.* **2007**, *46*, 3826.

[4] a) B. M. Weckhuysen, *Phys. Chem. Chem. Phys.* **2003**, *5*, 4351; J.-D. Grunwaldt, B. S. Clausen, *Top. Catal.* **2002**, *18*, 37; b) H. Topsøe, *J. Catal.* **2003**, *216*, 155.

[5] D. Koziej, M. Hubner, N. Barsan, U. Weimar, M. Sikora, J. D. Grunwaldt, *Phys. Chem. Chem. Phys.* **2009**, *11*, 8620.

[6] M. Gaidi, J. L. Hazemann, I. Matko, B. Chenevier, M. Rumyantseva, A. Gaskov, M. Labeau, *J. Electrochem. Soc.* **2000**, *147*, 3131.

[7] a) P. Glatzel, F. M. F. de Groot, O. Manoilova, D. Grandjean, B. M. Weckhuysen, U. Bergmann, R. Barrea, *Phys. Rev. B* **2005**, *772*, 014117; b) F. M. F. de Groot, A. Kotani, *Adv. Condens. Matter Sci.* **2008**, *6*, 259.

[8] a) K. Hamalainen, D. P. Siddons, J. B. Hastings, L. E. Berman, *Phys. Rev. Lett.* **1991**, *67*, 2850; b) P. Carra, M. Fabrizio, B. T. Thole, *Phys. Rev. Lett.* **1995**, *74*, 3700.

[9] A. Gurlo, R. Riedel, *ChemPhysChem* **2010**, *11*, 79.

[10] O. V. Safonova, M. Tromp, J. A. van Bokhoven, F. M. F. de Groot, J. Evans, P. Glatzel, *J. Phys. Chem. B* **2006**, *110*, 16162.

[11] J. Singh, E. M. C. Alayon, M. Tromp, O. V. Safonova, P. Glatzel, M. Nachtegaal, R. Frahm, J. A. van Bokhoven, *Angew. Chem.* **2008**, *120*, 9400; *Angew. Chem. Int. Ed.* **2008**, *47*, 9260.

[12] E. Bus, D. E. Ramaker, J. A. van Bokhoven, *J. Am. Chem. Soc.* **2007**, *129*, 8094.

[13] A. L. Ankudinov, J. J. Rehr, J. Low, S. R. Bare, *Phys. Rev. Lett.* **2001**, *86*, 1642.

[14] A. Cabot, J. Arbiol, J. R. Morante, U. Weimar, N. Barsan, W. Gopel, *Sens. Actuators B* **2000**, *70*, 87.

[15] V. A. Sole, C. Gauthier, J. Goulon, F. Natali, *J. Synchrotron Radiat.* **1999**, *6*, 174.

[16] P. Glatzel, U. Bergmann, *Coord. Chem. Rev.* **2005**, *249*, 65.

